Physica Scripta. Vol. 41, 134–139, 1990.

UV-Laserphotochemistry of Molecules on Solid Surfaces: NO/Ni(100)-O

Th. Mull, M. Menges, B. Baumeister, G. Odörfer, H. Geisler, G. Illing, R. M. Jaeger, H. Kuhlenbeck and H.-J. Freund

Physikalische Chemie I, Ruhr-Universität, D-4630 Bochum, FRG

D. Weide, U. Schüller and P. Andresen

Max-Planck-Institut für Strömungsforschung, D-3400 Göttingen, FRG

and

F. Budde, P. Ferm, V. Hamza and G. Ertl

Fritz-Haber-Institut der Max-Planck-Gesellschaft, D-1000 Berlin 33, FRG

Received July 16, 1989; accepted September 8, 1989

Abstract

We have studied the photochemistry of NO and NO_2 on Ni(100) using 193 nm light from an excimer laser. The experiment is complete in the sense that we characterize the desorbing particles by their rotationally and vibrationally resolved time of flight spectra via LIF (Laser Induced Fluorescence)- and REMPI (Resonance Enhanced Multi Photon Ionization)-techniques in the gas phase, and we characterize the solid surface before and after irradiation by electron spectroscopic methods, i.e., AES, LEED, and XPS.

We find the build up of NiO after irradiation of the molecular adsorbates. The structure of the oxide is characterized by LEED. The electronic and geometric structure of NO and NO_2 adsorbed on NiO is studied using angle resolved photoelectron spectroscopy (ARUPS), electron energy loss spectroscopy (HREELS) and near edge X-ray absorption fine structure (NEXAFS) measurements and the results are compared with those for NO and NO_2 on clean Ni(100). For the ARUPS and NEXAFS measurements we have used synchrotron radiation from the storage ring BESSY I in Berlin.

As expected, on NiO the desorption process has a much higher cross section than on the clean metal surface. A "photodesorption" channel of NO desorbing from NiO is clearly identified by the rotationally resolved time-of-flight spectra. In addition to the photodesorption channel a "thermal" channel is observed. The influence of the change of the adsorbate's geometric and electronic structure on desorption will be discussed.

1. Introduction

Only recently has the attention been turned to studies of UV-light induced photochemistry at well-characterized solid surfaces. Results have been presented for molecules on insulating [1–3], semiconducting [4–8] and metallic surfaces [9–33]. In order to undertake such studies it is desirable to look for the chemical changes on the solid surface, and at the same time to investigate desorbing particles in the gas phase above the surface.

The characterization of desorbing molecules may include the determination of the internal degrees of freedom, covering translational, rotational and vibrational properties. The chemical consequences of the photon induced reactions on the surface can be studied by electron spectroscopy, preferably HREELS, UPS, XPS and thermal desorption.

The conceptually simplest photochemical reaction occuring on a surface probably is the photolytic fission of the molecule-surface bond which may lead to desorption from the surface [21–23, 26–28]. The photolysis proceeds via electronic excitation of the adsorbate complex, and whether desorption occurs or not is controlled by energy dissipation processes into the solid [29, 30]. Particularly pathologic cases are metal surfaces which represent ideal sinks for electronic excitation energies because they basically accommodate any amount of energy via electron–hole–pair creation [29, 30]. Therefore, while clear evidences for photoinduced desorption processes do exist, these processes are far from being completely understood although considerable progress has been made in this respect in recent years [31]. On the other hand, it is much more likely to observe and study photoinduced processes from semiconductor surfaces because quenching of electronic excitations is much less likely to occur. We present in this study the results of the photochemical reactions of NO and NO_2 on Ni(100) at temperatures between $100\,K < T < 120\,K$. It is shown, that when NO and NO_2 are irradiated with light of 193 nm a thin NiO layer forms on the surface, from which NO desorbs with much higher yield as compared to the clean metal [20, 32]. We have characterized the NO and NO_2 adsorbate on the clean and the oxide covered metal surface via UPS, XPS, NEXAFS and HREELS and correlate the electronic and geometric structure of the molecules with the behaviour of the internal degrees of freedom of the desorbing molecules as determined via laser-induced fluorescence and resonant multi-photon-ionization.

2. Experimental

The results reported in the next section have been taken in two different UHV-systems. One [32] was equipped with a molecular beam, a rotable mass spectrometer for residual gas analysis and thermal desorption spectroscopy (TDS), and with facilities for low energy electron diffraction (LEED), Auger electron spectroscopy (AES), and argon ion bombardment.

The second system [33] contained facilities for X-ray photoelectron spectroscopy (XPS), LEED/AES and TDS.

The orientation of the (100) plane of the Ni sample was controlled by Laue diffraction. The sample was attached to a liquid nitrogen reservoir and could be cooled to 140 K (1. UHV system) and 90 K (2. UHV-system).

The sample was cleaned according to procedures reported in the literature [34, 35] until no impurities were detectable by

AES and XPS, respectively. Some measurements were carried out with a preoxidized surface which was obtained by dosing 300–400 L O_2 at $T = 400$ K. The desorption was initiated by an excimer laser (Lambda Physik EMG 200) which was run either in ArF ($\lambda = 193$ nm, $h\nu = 6.4$ eV) or KrF ($\lambda = 248$ nm, $h\nu = 5.0$ eV) mode with a pulse duration of 15 ns (FWHM). Using a diaphragm a beam of 10 mm diameter was created and directed onto the sample. Typically, the fluence was 2.5 mJ cm^{-2} per peak and the repetition rate was set at 10 Hz. Under these conditions, the calculated rase of the surface temperature during the laser pulse is smaller than 30 deg.

The desorbing molecules were measured by laser induced fluorescence or resonant multiphoton ionization as described in detail elsewhere [32].

3. Results and discussion

3.1. *NO/NiO(100)*

When a Ni(100) crystal is exposed to an NO-pressure of 10^{-7} torr, while the surface is irradiated by 193 nm laser light, a NiO film forms at the metal surface. From this oxide layer the desorption yield (10^{-2}) is considerably higher than from the clean metal surface, as we have reported earlier [26, 27, 32]. The transformation of an NO covered Ni(100) surface into NiO under the influence of laser irradiation is most probably not due to photodissociation of adsorbed NO but to adsorbed NO_2, which dissociates at low temperature upon adsorption into NO and oxygen, even without the influence of light. NO_2 often is a low concentration impurity in the NO gas used. The interaction of NO_2 with Ni(100) shall be discussed in part 2 of this chapter. In the following we report a more detailed characterization of the interaction of NO with a NiO surface in order to begin to understand the observed dissipation of the excitation energy into the internal degrees of freedom of the desorbing molecules, which has been reported earlier [26, 27, 32]. The surface we use has been prepared via thermal oxidation of the Ni(100) surface.

We know from earlier work [27, 32] that the thermal desorption spectrum for a laser oxidized surface is very similar to the desorption spectrum for a thermally oxidized surface. In the present study we have grown a thin epitaxial NiO layer on top of the Ni(100) surface. Figure 1 shows a set of LEED photographs taken during the process of growing the oxide layer. The first panel shows the clean Ni(100) substrate, the second panel a c(2 × 2) oxygen chemisorbate, and the third panel exhibits NiO(100) spots with residual c(2 × 2)O– and Ni(100)-spots. Further oxidation leads to pattern 1d where only NiO(100) spots can be identified. Due to a large density of defects these spots are rather broad. The thermal desorption spectrum taken on this substrate is compatible with the laser oxidized surface [27, 32], as shown in Fig. 2. The peak at 210 K shows a smaller width on the epitaxially grown layer and exhibits a rather wide shoulder at 240 K but basically no desorption signal in the region where desorption from the clean metal takes place (spectrum a). It is therefore reasonable to correlate the results gained on the NO adsorbate on top of an epitaxial NiO layer with those gained on the disordered oxide.

Briefly, we find bimodal time-of-flight distributions for the various rotational states of the desorbing molecules after irradiation with 226 nm [26, 27, 32]. As has been discussed in

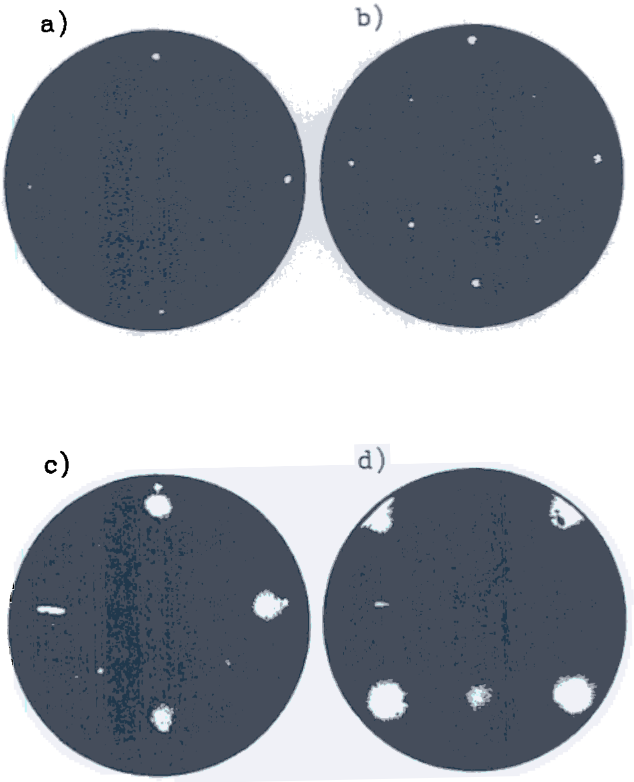

Fig. 1. LEED patterns observed on the clean and the oxidized Ni(100) surface. (a) Ni(100), clean surface, $E = 75$ eV. (b) c(2 × 2)O/Ni(100), $E = 68$ eV. (c) NiO(100)/Ni(100) with residual c(2 × 2)O– and Ni(100)-spots, $E = 68$ eV (d) NiO(100)/Ni(100), $E = 85$ eV.

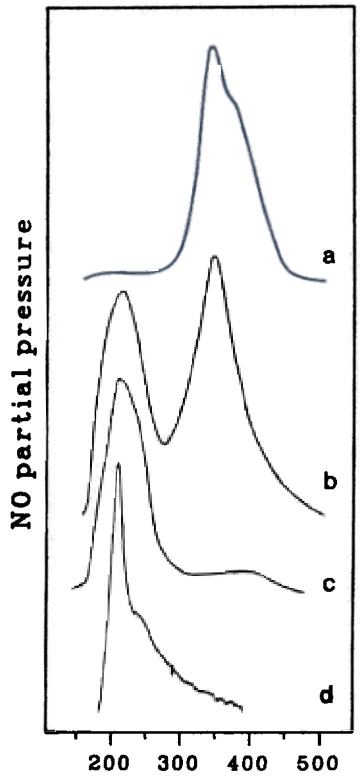

Fig. 2. Thermal desorption spectra of NO adsorbed on clean Ni(100) and on epitaxially grown NiO(100), prepared under various conditions. (a) NO desorbing from clean Ni(100). (b) NO desorbing from Ni(100) after prolonged laser irradiation of the NO adsorbate. After the irradiation the surface was redosed with NO. (c) NO desorbing from a oxygen predosed Ni(100) surface. (d) NO desorbing from epitaxially grown NiO(100)/Ni(100).

detail before [27, 32] we assign a "fast" channel to a true photodesorption channel, while a "slow" channel exhibits a behaviour which is in some respects characteristic for thermal desorption. For the "fast" channel we find an interesting behaviour, i.e., the internal rotational energy grows with increasing translational energy [27, 32]. This effect was also observed with other systems underoing photodesorption. The most striking manifestation of the non-thermal origin of the desorbing "fast" particles, however, stems from the observed spin–orbit selectivity [27]. We recall results shown in Fig. 3 whereafter desorption with $h\nu = 6.4\,\mathrm{eV}$ yields at low J'' predominantly particles in the $^2\Pi_{1/2}$-state, while at higher rotational energies both spin–orbit levels become equally populated. Such an effect had never been reported for systems either undergoing thermal desorption or direct inelastic scattering, although an experimental study belonging to the latter category [36, 37] prompted the development of a full quantum-mechanical theory for *scattering* of NO at a surface [38], the conclusions of which can be used for interpretation of the present findings.

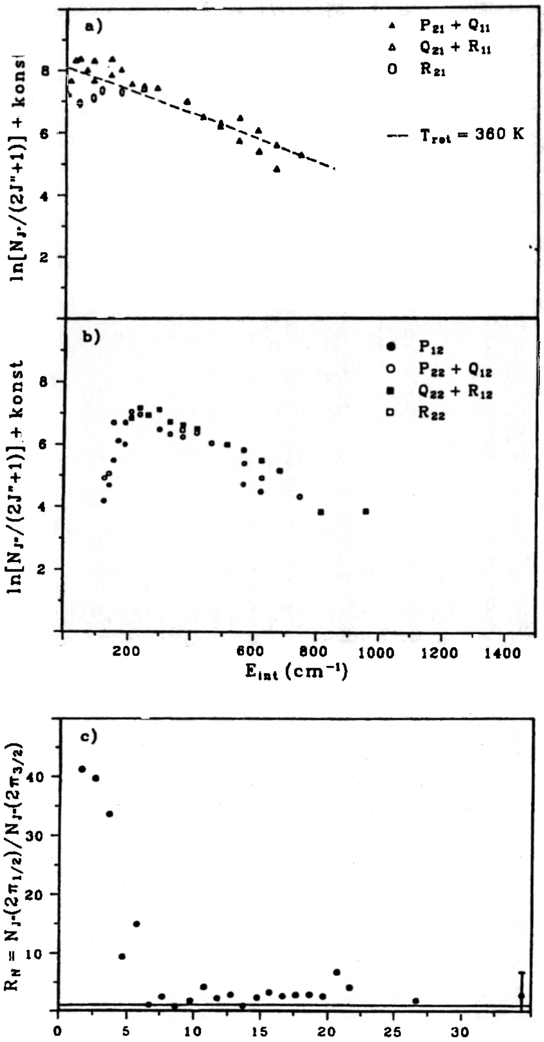

Fig. 3. (a) "Boltzmann plott", ln $[N_{J''}/(2J'' + 1)]$, vs. E_{int}, for the rotational population of the $2\pi_{1/2}$ manifold of "fast" NO molecules desorbing in the $v'' = 0$ level by 6.4 eV photons. The measured intensities reflecting the particle densities were converted into fluxes in order to take account of the fact, that the mean velocity varies with the rotational energy. (b) same as Fig. 3(a), but for the $2\pi_{3/2}$ manifold. (c) The population ratio $R_N = N_{J''}(2\pi_{1/2})/N_{J''}(2\pi_{3/2})$ of NO molecules photodesorbed by 6.4 eV photons in the $v'' = 0$ level.

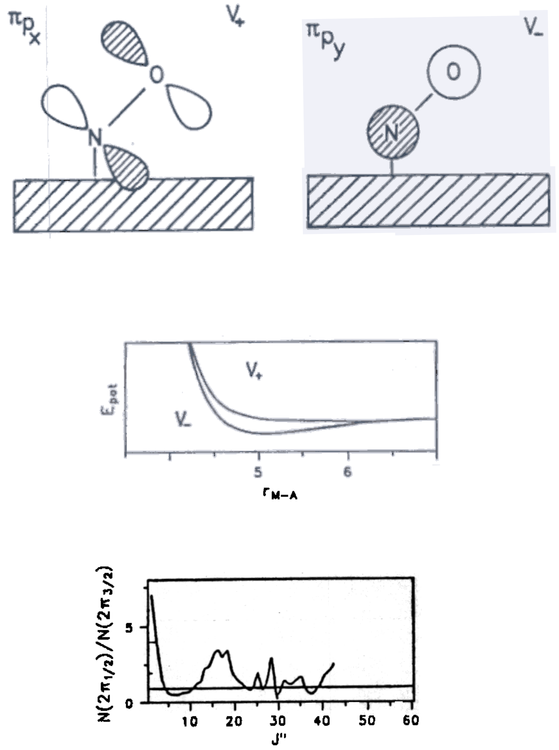

Fig. 4. The interaction potentials V_+ and V_- for a NO molecule inclined by 45° with respect to the surface normal with either the $2\pi^*p_x$ or $2\pi^*p_y$ orbital being singly occupied. The calculated population ratio $R_N = N(2\pi_{1/2})/N(2\pi_{3/2})$ for molecules scattered at these potentials exhibits a pronounced increase at low J'' values, in qualitative agreement with the experimental results shown in Fig. 10. After Smedley *et al.* [38].

The 2π-orbital of NO is singly occupied. If the axis of this molecule is parallel or inclined with respect to the surface, there will exist two interaction potentials with the surface, V_+ and V_-, depending on whether the singly occupied 2π-orbital is oriented perpendicular to the plane of symmetry spanned by the intermolecular axis and the surface normal. According to the theory by Smedley *et al.* [38], the existence of these two types of potentials will lead to non-equal populations of the two spin–orbit manifolds after scattering of NO at a rigid and flat surface. For the type of potentials V_+ and V_-, reproduced in Fig. 4, the calculated population ratio $N(^2\pi_{1/2})/N(^2\pi_{3/2})$ shows high values (corresponding to marked underpopulation of $^2\pi_{3/2}$) at low J''-values, while it rapidly levels off with increasing J''. The equal population of both spin–orbit manifolds at higher final rotational energy is due to a quantum-mechanical interference effect between the wave functions belonging to the two potentials V_+ and V_- which increases with increasing J''.

The sketched ideas may be adopted to the present case of photodesorption if this is considered to represent a half-collision in which the system starts to leave the surface from a point of the repulsive part of the interaction potential.

The key ingredient in order to understand the desorption behaviour is the ground state geometry of the adsorbed molecule. Therefore, we have characterized in greater detail the geometric and electronic structure of the NO adsorbate on the NiO surface. Figure 5α shows N1*s*-X-ray photoelectron spectra of NO on clean Ni(100) before and after heating the surface above room temperature, and of NO on NiO(100). The Ni(100) molecular chemisorbate shows a single, asymmetric peak, indicating a relatively strong elec-

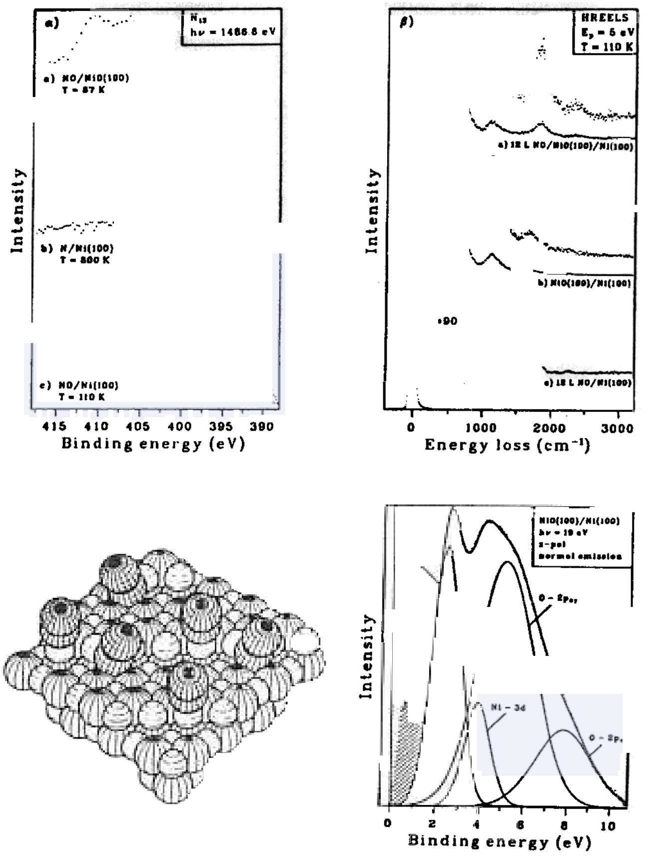

Fig. 5. Collection of electron spectroscopic data for NO/NiO(100)/Ni(100), NO/Ni(100) and NiO(100), and a plot showing some possible geometries for NO molecules adsorbing on surface defects on NiO(100). Panel α: collection of X-ray-photoelectron spectra of the N_{1s} level of adsorbed NO: (a) NO/Ni(100), $T = 115\,K$, (b) NO/Ni(100), annealed to $T = 800\,K$, (c) NO/NiO(100)Ni(100), $T = 115\,K$. Panel β: HREEL-spectra of adsorbed NO: (a) 12 L NO/NiO(100)/Ni(100), (b) NiO(100)/Ni(100), (c) 12 L NO/Ni(100). Panel γ: Structure plot showing some possible adsorption geometries of tilted NO adsorbed on defect sites on NiO(100). This plot should only be regarded as a tentative model. Panel δ: Fit of a photoelectron distribution of the valence bands of epitaxially grown NiO(100)/Ni(100). The ARUP-spectrum was taken in normal emission with Z-polarized light of $h\nu = 19\,eV$.

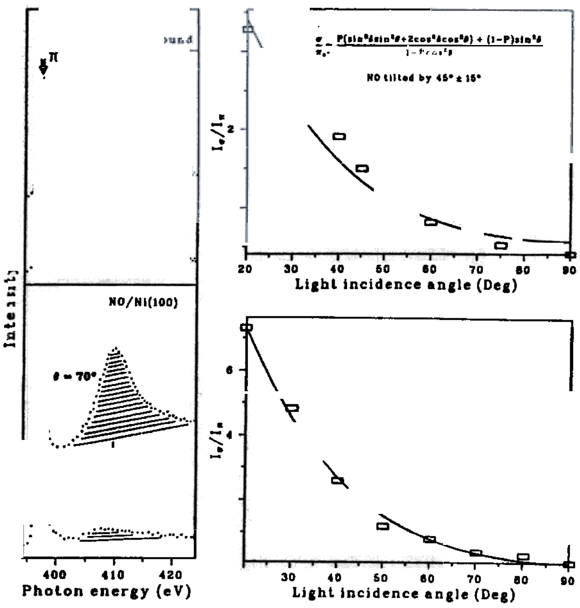

Fig. 6. N_{1s} NEXAF-spectra of NO adsorbed on epitaxially grown NiO(100) and on Ni(100) for two different polarizations of the incident light. In the right panel the intensity of the σ resonance is plotted vs. the angle of light incidence.

tronic molecule-surface coupling. Upon heating the molecules dissociate to form atomic nitrogen (and oxygen) with lower binding energy in the XPS-spectrum as compared to the molecular species. The spectrum of NO on NiO(100) on the other hand exhibits two peaks, typical for a weakly coupled system. The two lines represent the "screened", and the "unscreened" hole state of NO on the surface [39–42]. The latter state typically exhibits high intensities if the metal-molecule coupling is intermediate between chemisorption and physisorption [39–42], as for example in the cases of CO/Cu [43], and N_2/Ni [44]. HREELS measurements, collected in Fig. 5β reveal, that indeed there is only one type of species on the NiO surface with a vibrational frequency of 223 meV. This frequency is characteristic for NO adsorbed in "on-top" position (see the spectrum of NO on clean Ni(100) in Fig. 5β for comparison). Care has to be exercized when we compare properties of NO adsorbed on Ni, and on NiO because the electronic structure of the substrate has been considerably modified, i.e., we go from a metal to a semiconductor. A photoelectron spectrum (Fig. 5δ) of the epitaxially grown layer on top of the metal surface, which is still visible at the Fermi energy, shows that the Fermi energy of NiO is shifted by approximately 1.5 eV due to the existence of the band gap. The spectrum of the layer can be fitted rather satisfactorily by four components, the energies of which have been taken from photoelectron spectra of bulk NiO reported by Witzel *et al.* [45]. A more detailed investigation of the band dispersions in the NiO layer together with a more quantitative discussion of the line intensities allows to study the influence of defects present on the layer, as revealed by the rather extended LEED spots pictured in Fig. 1. This study shall be published elsewhere [46]. The important result for our present discussion of the desorption behaviour is the fact that NiO has a band gap. On such a surface quenching of excitations does not occur before the molecule has left it, so that the rather high desorption yield of 10^{-2} appears plausible.

The result most significant to understand the spin effect is shown in Fig. 6. There, the results of a NEXAFS study on the system NO/NiO(100), performed at the BESSY storage ring, are summarized. The left panel represents two spectra at normal and grazing incidence for the NO/NiO(100) system in comparison with the corresponding spectra of the system NO/Ni(100). In the left panels we have plotted the angular variations of the intensity ratio of the σ- and the π-resonance. Fitting the given formula (see the upper right panel of Fig. 6) we find a perpendicular orientation for NO/Ni(100), as already known for a long time [47], while it turns out that the molecular axis is inclined by 45° with respect to the surface normal on the oxide surface. In using this information for our discussion it has to be kept in mind that the oxidized surface contains more defects than the clean surface. It is therefore not clear whether the measured inclination angle refers to the local bonding geometry or whether it represents a global average. On the other hand, the observed spin effect can be taken as evidence for a bent adsorption geometry of NO on a NiO(100) surface, because after laser irrdiation the amount of adsorbed NO has decreased considerably, as revealed by thermal desorption and XPS.

Summarizing this section, we have characterized the NO adsorbate on the NiO(100) surface and find that the geometric

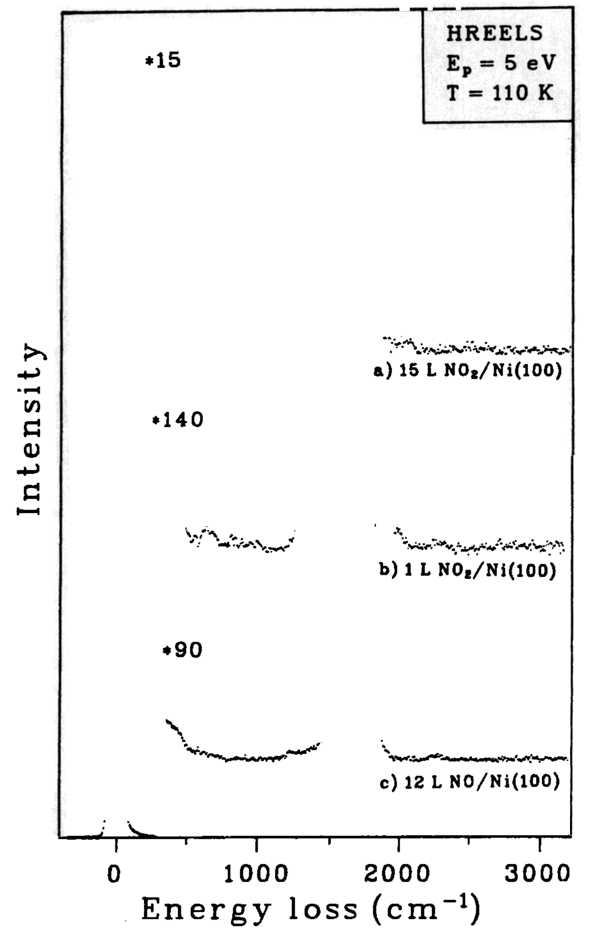

Fig. 7. HREEL-spectra of NO_2 and NO adsorbed on Ni(100): (a) 15 L NO_2/Ni(100), (b) 1 L NO_2/Ni(100), (c) 12 L NO/Ni(100).

and electronic structure of the adsorbate is compatible with the observed desorption behaviour. In particular, the observed spin effect may be a result of an inclined NO adsorbate geometry on the NiO surface as opposed to the perpendicular geometry found for the clean surface.

3.2. *NO_2/Ni(100)*

NO_2 does not adsorb molecularly on Ni(100) at any accessible temperature [48]. The HREELS spectra shown in Fig. 7 show that NO_2 dissociates into adsorbed oxygen and NO. Only at high NO_2 exposures we find a molecular species adsorbed either on top of the mixed O/NO layer or in separate islands. It appears very probable that the adsorbed molecular species is N_2O_4, i.e., the NO_2 dimer.

This particular adsorption behavior supports the statement made in the previous section, namely, that NO_2 may be responsible for the oxidation of the Ni(100) surface.

4. Summary and conclusion

Molecules undergoing photodesorption from a NiO(100) surface "remember" the potential they felt at the surface. We show that it is likely that NO molecules at a NiO surface are bound with their molecular axis inclined with respect to the surface normal. This finding allows us to describe the unusual underpopulation of the $^2\pi_{3/2}$ state for the desorbing NO molecules at low rotational energies in terms of a theory developed by Smedley *et al.* taking the coupling of the electronic state and the nuclear motion upon desorption into account.

Acknowledgements

We are grateful to the Deutsche Forschungsgemeinschaft as well as to the Ministerium für Wissenschaft und Forschung des Landes Nordrhein-Westfalen for financial support.

References

1. Bourdon, E. B. D., Das, P., Harrison, I., Polanyi, J. C., Segner, J., et al., Faraday Discuss. Chem. Soc. **82**, 343 (1986).
2. Bourdon, E. B. D., Cowin, J. P., Harrison, I., Polanyi, J. C., Segner, J. *et al.*, J. Phys. Chem. **88**, 6100 (1984).
3. Tabares, F. L., Marsh, E. P., Bach, G. A. and Cowin, J. P., J. Chem. Phys. **86**, 738 (1987).
4. Swanson, J. R., Friend, C. M. and Chabal, Y. J., J. Chem. Phys. **87**, 5028 (1987).
5. Creighton, J. R., J. Vac. Sci. Technol. **A4**, 669 (1986).
6. Ho, W., Comments Cond. Mater. Phys. **13**, 293 (1988).
7. Marsh, E. P., Tabares, F. L., Schneider, M. R. and Cowin, J. P., J. Vac. Sci. Technol. **A5**, 519 (1987).
8. Ying, Z. and Ho, W., Phys. Rev. Lett. **60** (1988) 57.
9. Marsh, E. P., Tabares, F. L., Schneider, M. R. and Cowin, J. P., in Chemically Modified Surfaces (Edited by D. Leyden), Gordon and Breach, New York (1988).
10. Marsh, E. P., Schneider, M. R., Gilton, T. L., Tabares, F. L., Meier, W. and Cowin, J. P., Phys. Rev. Lett. **60**, 2551 (1988).
11. Celli, F. G., Whitmore, P. M. and Janda, K. C., Chem. Phys. Lett. **138**, 257 (1987).
12. Domen, K. and Chuang, T. J., Phys. Rev. Lett. **59**, 1484 (1987).
13. Grassian, V. H. and Pimentel, G. C., J. Chem. Phys. **88**, 4478 (1988).
14. Grassian, V. H. and Pimentel, G. C., J. Chem. Phys. **88**, 4484 (1988).
15. Roop, B., Costello, S. A., Greenlief, C. M. and White, J. M., Chem. Phys. Lett. **143**, 38 (1988).
16. Costello, S. A., Roop, B., Liu, Z.-M. and White, J. M., J. Phys. Chem. **92**, 1019 (1988).
17. Zhou, Y., Feng, W. M., Henderson, M. A., Roop, B. and White, J. M., J. Am. Chem. Soc. **110**, 4447 (1988).
18. Roop, B., Costello, S. A., Liu, Z.-M. and White, J. M. in Proceedings of the XIX Solvay Conference, (Edited by F. W. deWette) Springer, New York, (1988), p. 343.
19. Liu, Z.-M., Akhter, S., Roop, B. and White, J. M. J. Am. Chem. Soc. **110**, 8708 (1988).
20. Germer, Th. A., Ho, W., J. Vac. Sci. Technol. **A7**, 1878 (1989).
21. Burgess, Jr. D., Mantell, D. A., Cavanagh, R. R. and King, D. S., J. Chem. Phys. **85**, 3123 (1986).
22. Burgess, Jr. D., Cavanagh, R. R. and King, D. S., J. Chem. Phys. **88**, 6556 (1988).
23. Buntin, S. A., Richter, L. J., Cavanagh, R. R. and King, D. S., Phys. Rev. Lett. **61**, 1321 (1988).
24. Hoheisel, W., Jungmann, K., Vollmer, M., Weidenauer, R. and Träger, F., Phys. Rev. Lett. **60**, 1649 (1988).
25. Natzle, W. C., Padowitz, D. and Sibener, S. J., J. Chem. Phys. **88**, 7975 (1988).
26. Weide, D., Andresen, P. and Freund, H.-J., Chem. Phys. Lett. **136**, 107 (1987).
27. Budde, F., Hamza, A. V., Ferm, P. M., Ertl, G., Weide, D., Andresen, P. and Freund, H.-J., Phys. Rev. Lett. **60**, 1518 (1988).
28. (a) Menzel, D. and Gomer, R., J. Chem. Phys. **41**, 3311 (1964); (b) Readhead, P. A., Can. J. Phys. **42**, 886 (1964).
29. Menzel, D., Nucl. Instr. Meth. **B13**, 507 (1986).
30. Menzel, D., in "Study of Surfaces and Interfaces by Electron Optical Techniques" (Edited by A. Howie and U. Valdre), Plenum Press, New York (1988).
31. Desorption Induced by Electronic Transitions, Diet III, Stulen, R. H., Knotek, M. L., (Eds.) in Springer Series in Surface Sciences **13**, Springer, New York, (1988).
32. Ferm, P. M., Budde, F., Hamza, A. V., Jakubith, S., Ertl, G., Weide, D., Andresen, P., Freund, H.-J., Surf. Sci., to be published.
33. Mull, Th. Dissertation, Bochum (in progress).
34. Koel, B. E., Peebles, D. E. and White, J. M., Surf. Sci. **125**, 709 (1983).
35. Dalmai-Imelik, G., Bertolini, J. C. and Rousseau, J., Surf. Sci. **63**, 67 (1977).

36. Cowin, J. P., Auerbach, D. J., Becker, C. and Wharton, L., Surf. Sci. **78** (1978) 545.
37. Cowin, J. P., Phys. Rev. Lett. **54**, 368 (1985).
38. Smedley, J., Corey, G. C. and Alexander, M. H., J. Chem. Phys. **87**, 3218 (1987).
39. Schönhammer, K. and Gunnarsson, O., Solid State Commun. **26**, 399 (1978).
40. Hermann, K., Bagus, P. S., Brundle, C. R. and Menzel, D., Phys. Rev. **B24**, 7025 (1981).
41. Freund, H.-J., and Plummer, E. W., Phys. Rev. **B23**, 4859 (1981).
42. Messmer, R. P., and Lamson, S. H., Chem. Phys. Lett. **65** 465 (1979).
43. Brundle, C. R. and Wandelt, K. Proc. 7th Int. Vac. Congr., Vienna, p. 1171 (1977).
44. Fuggle, J. C., Umbach, E., Menzel, D., Wandelt, F. and Brundle, C. R. Solid State Commun. **27**, 65 (1978).
45. Witzel, S. and Neumann, M., to be published; see also BESSY-Jahresbericht p. 197 (1988).
46. Odörfer, G., Kuhlenbeck, H. and Freund, H.-J., unpublished.
47. Stöhr, J. and Jaeger, R., Phys. Rev. **B26**, 4111 (1982).
48. Geisler, H., Diplomarbeit, Bochum (1989).

~~100~~ 99

Physica Scripta. Vol. 41, 134–139, 1990.

UV-Laserphotochemistry of Molecules on Solid Surfaces: NO/Ni(100)-O

Th. Mull, M. Menges, B. Baumeister, G. Odörfer, H. Geisler, G. Illing, R. M. Jaeger, H. Kuhlenbeck and H.-J. Freund

Physikalische Chemie I, Ruhr-Universität, D-4630 Bochum, FRG

D. Weide, U. Schüller and P. Andresen

Max-Planck-Institut für Strömungsforschung, D-3400 Göttingen, FRG

and

F. Budde, P. Ferm, V. Hamza and G. Ertl

Fritz-Haber-Institut der Max-Planck-Gesellschaft, D-1000 Berlin 33, FRG

Received July 16, 1989; accepted September 8, 1989

Abstract

We have studied the photochemistry of NO and NO_2 on Ni(100) using 193 nm light from an excimer laser. The experiment is complete in the sense that we characterize the desorbing particles by their rotationally and vibrationally resolved time of flight spectra via LIF (Laser Induced Fluorescence)- and REMPI (Resonance Enhanced Multi Photon Ionization)-techniques in the gas phase, and we characterize the solid surface before and after irradiation by electron spectroscopic methods, i.e., AES, LEED, and XPS.

We find the build up of NiO after irradiation of the molecular adsorbates. The structure of the oxide is characterized by LEED. The electronic and geometric structure of NO and NO_2 adsorbed on NiO is studied using angle resolved photoelectron spectroscopy (ARUPS), electron energy loss spectroscopy (HREELS) and near edge X-ray absorption fine structure (NEXAFS) measurements and the results are compared with those for NO and NO_2 on clean Ni(100). For the ARUPS and NEXAFS measurements we have used synchrotron radiation from the storage ring BESSY I in Berlin.

As expected, on NiO the desorption process has a much higher cross section than on the clean metal surface. A "photodesorption" channel of NO desorbing from NiO is clearly identified by the rotationally resolved time-of-flight spectra. In addition to the photodesorption channel a "thermal" channel is observed. The influence of the change of the adsorbate's geometric and electronic structure on desorption will be discussed.

1. Introduction

Only recently has the attention been turned to studies of UV-light induced photochemistry at well-characterized solid surfaces. Results have been presented for molecules on insulating [1–3], semiconducting [4–8] and metallic surfaces [9–33]. In order to undertake such studies it is desirable to look for the chemical changes on the solid surface, and at the same time to investigate desorbing particles in the gas phase above the surface.

The characterization of desorbing molecules may include the determination of the internal degrees of freedom, covering translational, rotational and vibrational properties. The chemical consequences of the photon induced reactions on the surface can be studied by electron spectroscopy, preferably HREELS, UPS, XPS and thermal desorption.

The conceptually simplest photochemical reaction occuring on a surface probably is the photolytic fission of the molecule-surface bond which may lead to desorption from the surface [21–23, 26–28]. The photolysis proceeds via electronic excitation of the adsorbate complex, and whether desorption occurs or not is controlled by energy dissipation processes into the solid [29, 30]. Particularly pathologic cases are metal surfaces which represent ideal sinks for electronic excitation energies because they basically accommodate any amount of energy via electron–hole–pair creation [29, 30]. Therefore, while clear evidences for photoinduced desorption processes do exist, these processes are far from being completely understood although considerable progress has been made in this respect in recent years [31]. On the other hand, it is much more likely to observe and study photoinduced processes from semiconductor surfaces because quenching of electronic excitations is much less likely to occur. We present in this study the results of the photochemical reactions of NO and NO_2 on Ni(100) at temperatures between $100\,K < T < 120\,K$. It is shown, that when NO and NO_2 are irradiated with light of 193 nm a thin NiO layer forms on the surface, from which NO desorbs with much higher yield as compared to the clean metal [20, 32]. We have characterized the NO and NO_2 adsorbate on the clean and the oxide covered metal surface via UPS, XPS, NEXAFS and HREELS and correlate the electronic and geometric structure of the molecules with the behaviour of the internal degrees of freedom of the desorbing molecules as determined via laser-induced fluorescence and resonant multi-photon-ionization.

2. Experimental

The results reported in the next section have been taken in two different UHV-systems. One [32] was equipped with a molecular beam, a rotable mass spectrometer for residual gas analysis and thermal desorption spectroscopy (TDS), and with facilities for low energy electron diffraction (LEED), Auger electron spectroscopy (AES), and argon ion bombardment.

The second system [33] contained facilities for X-ray photoelectron spectroscopy (XPS), LEED/AES and TDS.

The orientation of the (100) plane of the Ni sample was controlled by Laue diffraction. The sample was attached to a liquid nitrogen reservoir and could be cooled to 140 K (1. UHV system) and 90 K (2. UHV-system).

The sample was cleaned according to procedures reported in the literature [34, 35] until no impurities were detectable by

AES and XPS, respectively. Some measurements were carried out with a preoxidized surface which was obtained by dosing 300–400 L O_2 at T = 400 K. The desorption was initiated by an excimer laser (Lambda Physik EMG 200) which was run either in ArF (λ = 193 nm, $h\nu$ = 6.4 eV) or KrF (λ = 248 nm, $h\nu$ = 5.0 eV) mode with a pulse duration of 15 ns (FWHM). Using a diaphragm a beam of 10 mm diameter was created and directed onto the sample. Typically, the fluence was 2.5 mJ cm^{-2} per peak and the repetition rate was set at 10 Hz. Under these conditions, the calculated rase of the surface temperature during the laser pulse is smaller than 30 deg.

The desorbing molecules were measured by laser induced fluorescence or resonant multiphoton ionization as described in detail elsewhere [32].

3. Results and discussion

3.1. *NO/NiO(100)*

When a Ni(100) crystal is exposed to an NO-pressure of 10^{-7} torr, while the surface is irradiated by 193 nm laser light, a NiO film forms at the metal surface. From this oxide layer the desorption yield (10^{-2}) is considerably higher than from the clean metal surface, as we have reported earlier [26, 27, 32]. The transformation of an NO covered Ni(100) surface into NiO under the influence of laser irradiation is most probably not due to photodissociation of adsorbed NO but to adsorbed NO_2, which dissociates at low temperature upon adsorption into NO and oxygen, even without the influence of light. NO_2 often is a low concentration impurity in the NO gas used. The interaction of NO_2 with Ni(100) shall be discussed in part 2 of this chapter. In the following we report a more detailed characterization of the interaction of NO with a NiO surface in order to begin to understand the observed dissipation of the excitation energy into the internal degrees of freedom of the desorbing molecules, which has been reported earlier [26, 27, 32]. The surface we use has been prepared via thermal oxidation of the Ni(100) surface.

We know from earlier work [27, 32] that the thermal desorption spectrum for a laser oxidized surface is very similar to the desorption spectrum for a thermally oxidized surface. In the present study we have grown a thin epitaxial NiO layer on top of the Ni(100) surface. Figure 1 shows a set of LEED photographs taken during the process of growing the oxide layer. The first panel shows the clean Ni(100) substrate, the second panel a c(2 × 2) oxygen chemisorbate, and the third panel exhibits NiO(100) spots with residual c(2 × 2)O- and Ni(100)-spots. Further oxidation leads to pattern 1d where only NiO(100) spots can be identified. Due to a large density of defects these spots are rather broad. The thermal desorption spectrum taken on this substrate is compatible with the laser oxidized surface [27, 32], as shown in Fig. 2. The peak at 210 K shows a smaller width on the epitaxially grown layer and exhibits a rather wide shoulder at 240 K but basically no desorption signal in the region where desorption from the clean metal takes place (spectrum a). It is therefore reasonable to correlate the results gained on the NO adsorbate on top of an epitaxial NiO layer with those gained on the disordered oxide.

Briefly, we find bimodal time-of-flight distributions for the various rotational states of the desorbing molecules after irradiation with 226 nm [26, 27, 32]. As has been discussed in

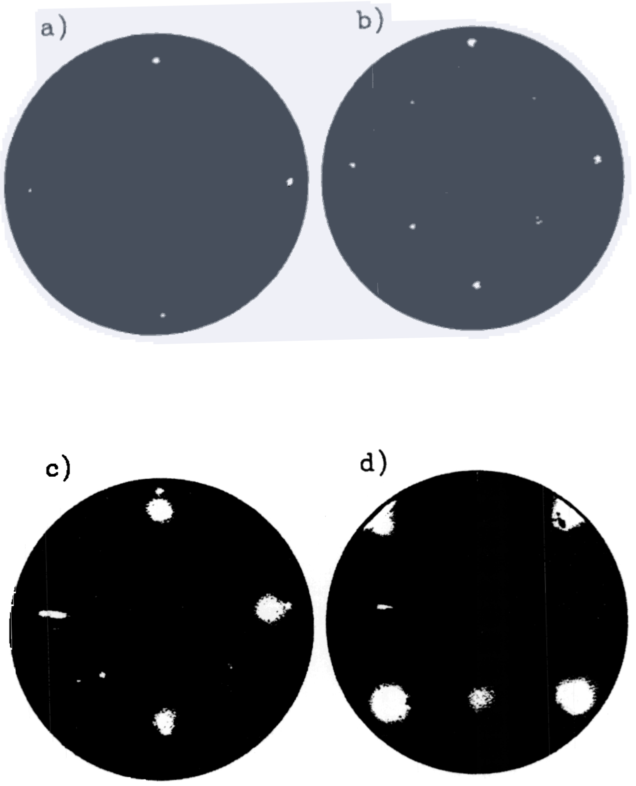

Fig. 1. LEED patterns observed on the clean and the oxidized Ni(100) surface. (a) Ni(100), clean surface, E = 75 eV. (b) c(2 × 2)O/Ni(100), E = 68 eV. (c) NiO(100)/Ni(100) with residual c(2 × 2)O- and Ni(100)-spots, E = 68 eV (d) NiO(100)/Ni(100), E = 85 eV.

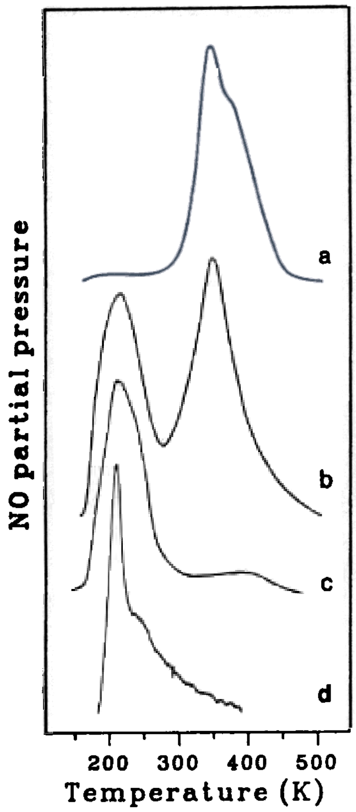

Fig. 2. Thermal desorption spectra of NO adsorbed on clean Ni(100) and on epitaxially grown NiO(100), prepared under various conditions. (a) NO desorbing from clean Ni(100). (b) NO desorbing from Ni(100) after prolonged laser irradiation of the NO adsorbate. After the irradiation the surface was redosed with NO. (c) NO desorbing from a oxygen predosed Ni(100) surface. (d) NO desorbing from epitaxially grown NiO(100)/Ni(100).

detail before [27, 32] we assign a "fast" channel to a true photodesorption channel, while a "slow" channel exhibits a behaviour which is in some respects characteristic for thermal desorption. For the "fast" channel we find an interesting behaviour, i.e., the internal rotational energy grows with increasing translational energy [27, 32]. This effect was also observed with other systems underoing photodesorption. The most striking manifestation of the non-thermal origin of the desorbing "fast" particles, however, stems from the observed spin–orbit selectivity [27]. We recall results shown in Fig. 3 whereafter desorption with $h\nu = 6.4\,\mathrm{eV}$ yields at low J'' predominantly particles in the $^2\Pi_{1/2}$-state, while at higher rotational energies both spin–orbit levels become equally populated. Such an effect had never been reported for systems either undergoing thermal desorption or direct inelastic scattering, although an experimental study belonging to the latter category [36, 37] prompted the development of a full quantum-mechanical theory for *scattering* of NO at a surface [38], the conclusions of which can be used for interpretation of the present findings.

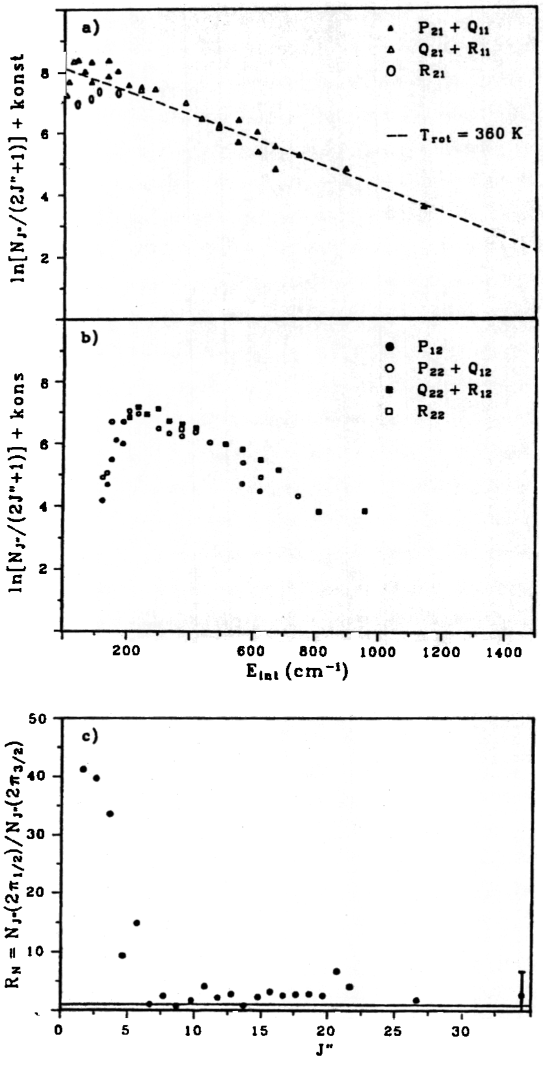

Fig. 3. (a) "Boltzmann plott", $\ln[N_{J''}/(2J'' + 1)]$, vs. E_{int}, for the rotational population of the $2\pi_{1/2}$ manifold of "fast" NO molecules desorbing in the $v'' = 0$ level by 6.4 eV photons. The measured intensities reflecting the particle densities were converted into fluxes in order to take account of the fact, that the mean velocity varies with the rotational energy. (b) same as Fig. 3(a), but for the $2\pi_{3/2}$ manifold. (c) The population ratio $R_N = N_{J''}(2\pi_{1/2})/N_{J''}(2\pi_{3/2})$ of NO molecules photodesorbed by 6.4 eV photons in the $v'' = 0$ level.

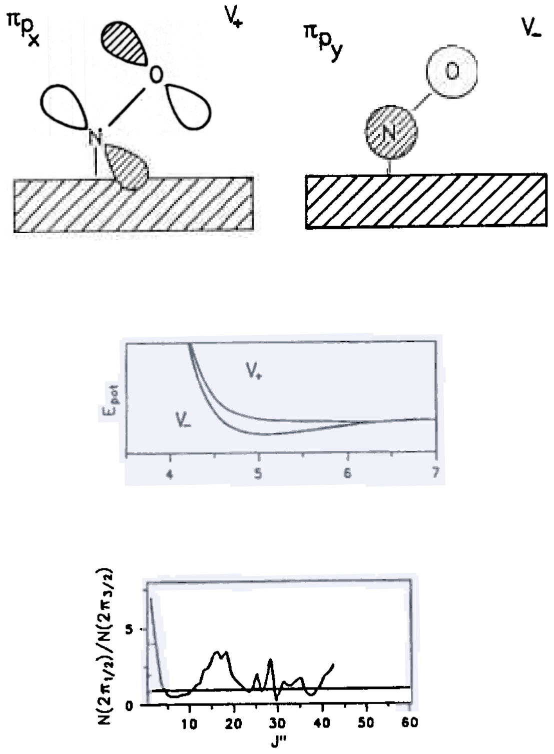

Fig. 4. The interaction potentials V_+ and V_- for a NO molecule inclined by 45° with respect to the surface normal with either the $2\pi^*p_x$ or $2\pi^*p_y$ orbital being singly occupied. The calculated population ratio $R_N = N(2\pi_{1/2})/N(2\pi_{3/2})$ for molecules scattered at these potentials exhibits a pronounced increase at low J'' values, in qualitative agreement with the experimental results shown in Fig. 10. After Smedley *et al.* [38].

The 2π-orbital of NO is singly occupied. If the axis of this molecule is parallel or inclined with respect to the surface, there will exist two interaction potentials with the surface, V_+ and V_-, depending on whether the singly occupied 2π-orbital is oriented perpendicular to the plane of symmetry spanned by the intermolecular axis and the surface normal. According to the theory by Smedley *et al.* [38], the existence of these two types of potentials will lead to non-equal populations of the two spin–orbit manifolds after scattering of NO at a rigid and flat surface. For the type of potentials V_+ and V_-, reproduced in Fig. 4, the calculated population ratio $N(^2\pi_{1/2})/N(^2\pi_{3/2})$ shows high values (corresponding to marked underpopulation of $^2\pi_{3/2}$) at low J''-values, while it rapidly levels off with increasing J''. The equal population of both spin–orbit manifolds at higher final rotational energy is due to a quantum-mechanical interference effect between the wave functions belonging to the two potentials V_+ and V_- which increases with increasing J''.

The sketched ideas may be adopted to the present case of photodesorption if this is considered to represent a half-collision in which the system starts to leave the surface from a point of the repulsive part of the interaction potential.

The key ingredient in order to understand the desorption behaviour is the ground state geometry of the adsorbed molecule. Therefore, we have characterized in greater detail the geometric and electronic structure of the NO adsorbate on the NiO surface. Figure 5*a* shows N1*s*-X-ray photoelectron spectra of NO on clean Ni(100) before and after heating the surface above room temperature, and of NO on NiO(100). The Ni(100) molecular chemisorbate shows a single, asymmetric peak, indicating a relatively strong elec-

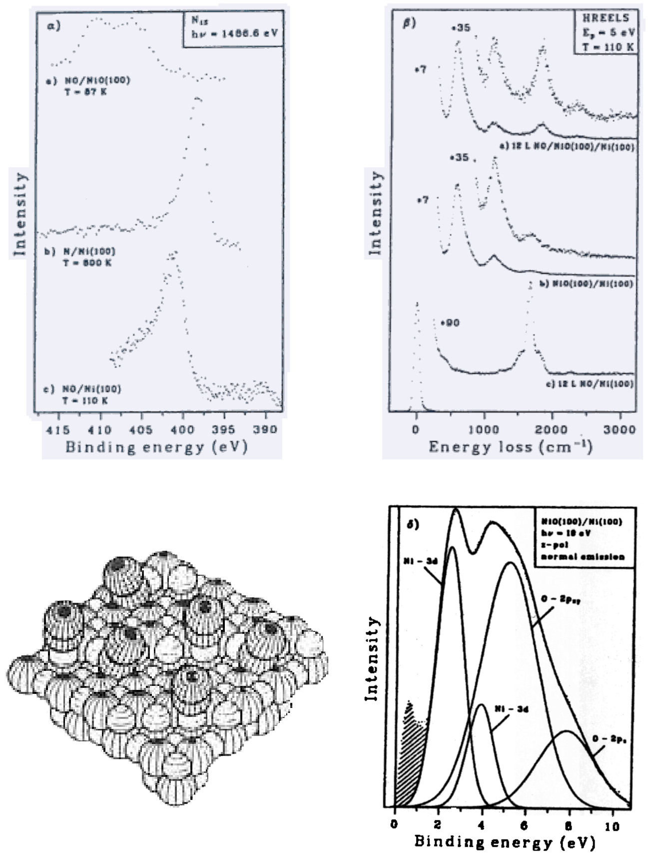

Fig. 5. Collection of electron spectroscopic data for NO/NiO(100)/Ni(100), NO/Ni(100) and NiO(100), and a plot showing some possible geometries for NO molecules adsorbing on surface defects on NiO(100). Panel α: collection of X-ray-photoelectron spectra of the N_{1s} level of adsorbed NO: (a) NO/Ni(100), $T = 115$ K, (b) NO/Ni(100), annealed to $T = 800$ K, (c) NO/NiO(100)Ni(100), $T = 115$ K. Panel β: HREEL-spectra of adsorbed NO: (a) 12 L NO/NiO(100)/Ni(100), (b) NiO(100)/Ni(100), (c) 12 L NO/Ni(100). Panel γ: Structure plot showing some possible adsorption geometries of tilted NO adsorbed on defect sites on NiO(100). This plot should only be regarded as a tentative model. Panel δ: Fit of a photoelectron distribution of the valence bands of epitaxially grown NiO(100)/Ni(100). The ARUP-spectrum was taken in normal emission with Z-polarized light of $h\nu = 19$ eV.

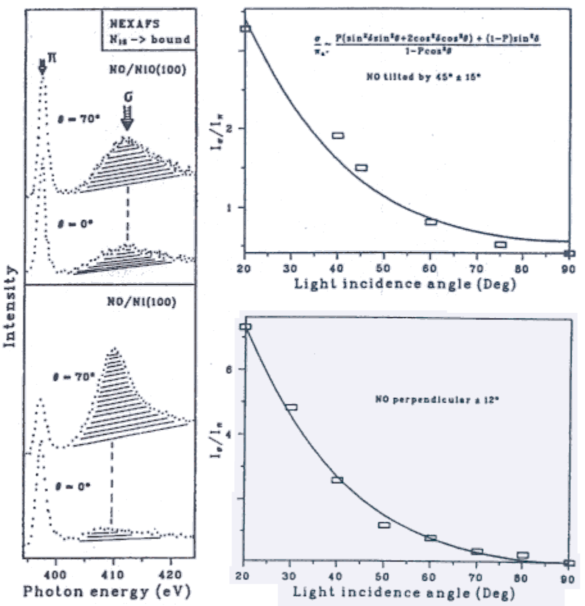

Fig. 6. N_{1s} NEXAF-spectra of NO adsorbed on epitaxially grown NiO(100) and on Ni(100) for two different polarizations of the incident light. In the right panel the intensity of the σ resonance is plotted vs. the angle of light incidence.

tronic molecule-surface coupling. Upon heating the molecules dissociate to form atomic nitrogen (and oxygen) with lower binding energy in the XPS-spectrum as compared to the molecular species. The spectrum of NO on NiO(100) on the other hand exhibits two peaks, typical for a weakly coupled system. The two lines represent the "screened", and the "unscreened" hole state of NO on the surface [39–42]. The latter state typically exhibits high intensities if the metal-molecule coupling is intermediate between chemisorption and physisorption [39–42], as for example in the cases of CO/Cu [43], and N_2/Ni [44]. HREELS measurements, collected in Fig. 5β reveal, that indeed there is only one type of species on the NiO surface with a vibrational frequency of 223 meV. This frequency is characteristic for NO adsorbed in "on-top" position (see the spectrum of NO on clean Ni(100) in Fig. 5β for comparison). Care has to be exercized when we compare properties of NO adsorbed on Ni, and on NiO because the electronic structure of the substrate has been considerably modified, i.e., we go from a metal to a semiconductor. A photoelectron spectrum (Fig. 5δ) of the epitaxially grown layer on top of the metal surface, which is still visible at the Fermi energy, shows that the Fermi energy of NiO is shifted by approximately 1.5 eV due to the existence of the band gap. The spectrum of the layer can be fitted rather satisfactorily by four components, the energies of which have been taken from photoelectron spectra of bulk NiO reported by Witzel *et al.* [45]. A more detailed investigation of the band dispersions in the NiO layer together with a more quantitative discussion of the line intensities allows to study the influence of defects present on the layer, as revealed by the rather extended LEED spots pictured in Fig. 1. This study shall be published elsewhere [46]. The important result for our present discussion of the desorption behaviour is the fact that NiO has a band gap. On such a surface quenching of excitations does not occur before the molecule has left it, so that the rather high desorption yield of 10^{-2} appears plausible.

The result most significant to understand the spin effect is shown in Fig. 6. There, the results of a NEXAFS study on the system NO/NiO(100), performed at the BESSY storage ring, are summarized. The left panel represents two spectra at normal and grazing incidence for the NO/NiO(100) system in comparison with the corresponding spectra of the system NO/Ni(100). In the left panels we have plotted the angular variations of the intensity ratio of the σ- and the π-resonance. Fitting the given formula (see the upper right panel of Fig. 6) we find a perpendicular orientation for NO/Ni(100), as already known for a long time [47], while it turns out that the molecular axis is inclined by 45° with respect to the surface normal on the oxide surface. In using this information for our discussion it has to be kept in mind that the oxidized surface contains more defects than the clean surface. It is therefore not clear whether the measured inclination angle refers to the local bonding geometry or whether it represents a global average. On the other hand, the observed spin effect can be taken as evidence for a bent adsorption geometry of NO on a NiO(100) surface, because after laser irrdiation the amount of adsorbed NO has decreased considerably, as revealed by thermal desorption and XPS.

Summarizing this section, we have characterized the NO adsorbate on the NiO(100) surface and find that the geometric

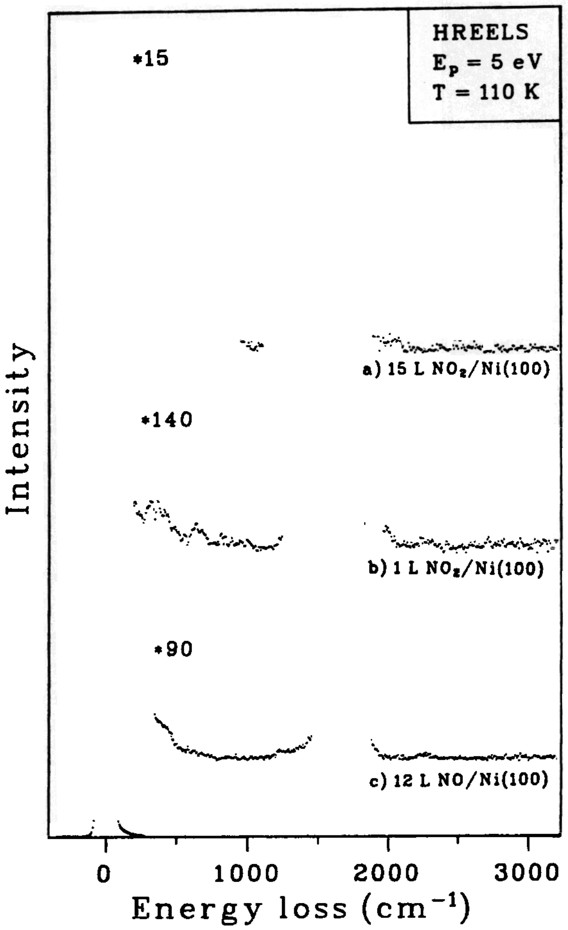

Fig. 7. HREEL-spectra of NO_2 and NO adsorbed on Ni(100): (a) 15 L NO_2/Ni(100), (b) 1 L NO_2/Ni(100), (c) 12 L NO/Ni(100).

and electronic structure of the adsorbate is compatible with the observed desorption behaviour. In particular, the observed spin effect may be a result of an inclined NO adsorbate geometry on the NiO surface as opposed to the perpendicular geometry found for the clean surface.

3.2. *NO_2/Ni(100)*

NO_2 does not adsorb molecularly on Ni(100) at any accessible temperature [48]. The HREELS spectra shown in Fig. 7 show that NO_2 dissociates into adsorbed oxygen and NO. Only at high NO_2 exposures we find a molecular species adsorbed either on top of the mixed O/NO layer or in separate islands. It appears very probable that the adsorbed molecular species is N_2O_4, i.e., the NO_2 dimer.

This particular adsorption behavior supports the statement made in the previous section, namely, that NO_2 may be responsible for the oxidation of the Ni(100) surface.

4. Summary and conclusion

Molecules undergoing photodesorption from a NiO(100) surface "remember" the potential they felt at the surface. We show that it is likely that NO molecules at a NiO surface are bound with their molecular axis inclined with respect to the surface normal. This finding allows us to describe the unusual underpopulation of the $^2\pi_{3/2}$ state for the desorbing NO molecules at low rotational energies in terms of a theory developed by Smedley *et al.* taking the coupling of the electronic state and the nuclear motion upon desorption into account.

Acknowledgements

We are grateful to the Deutsche Forschungsgemeinschaft as well as to the Ministerium für Wissenschaft und Forschung des Landes Nordrhein-Westfalen for financial support.

References

1. Bourdon, E. B. D., Das, P., Harrison, I., Polanyi, J. C., Segner, J., et al., Faraday Discuss. Chem. Soc. **82**, 343 (1986).
2. Bourdon, E. B. D., Cowin, J. P., Harrison, I., Polanyi, J. C., Segner, J. *et al.*, J. Phys. Chem. **88**, 6100 (1984).
3. Tabares, F. L., Marsh, E. P., Bach, G. A. and Cowin, J. P., J. Chem. Phys. **86**, 738 (1987).
4. Swanson, J. R., Friend, C. M. and Chabal, Y. J., J. Chem. Phys. **87**, 5028 (1987).
5. Creighton, J. R., J. Vac. Sci. Technol. **A4**, 669 (1986).
6. Ho, W., Comments Cond. Mater. Phys. **13**, 293 (1988).
7. Marsh, E. P., Tabares, F. L., Schneider, M. R. and Cowin, J. P., J. Vac. Sci. Technol. **A5**, 519 (1987).
8. Ying, Z. and Ho, W., Phys. Rev. Lett. **60** (1988) 57.
9. Marsh, E. P., Tabares, F. L., Schneider, M. R. and Cowin, J. P., in Chemically Modified Surfaces (Edited by D. Leyden), Gordon and Breach, New York (1988).
10. Marsh, E. P., Schneider, M. R., Gilton, T. L., Tabares, F. L., Meier, W. and Cowin, J. P., Phys. Rev. Lett. **60**, 2551 (1988).
11. Celli, F. G., Whitmore, P. M. and Janda, K. C., Chem. Phys. Lett. **138**, 257 (1987).
12. Domen, K. and Chuang, T. J., Phys. Rev. Lett. **59**, 1484 (1987).
13. Grassian, V. H. and Pimentel, G. C., J. Chem. Phys. **88**, 4478 (1988).
14. Grassian, V. H. and Pimentel, G. C., J. Chem. Phys. **88**, 4484 (1988).
15. Roop, B., Costello, S. A., Greenlief, C. M. and White, J. M., Chem. Phys. Lett. **143**, 38 (1988).
16. Costello, S. A., Roop, B., Liu, Z.-M. and White, J. M., J. Phys. Chem. **92**, 1019 (1988).
17. Zhou, Y., Feng, W. M., Henderson, M. A., Roop, B. and White, J. M., J. Am. Chem. Soc. **110**, 4447 (1988).
18. Roop, B., Costello, S. A., Liu, Z.-M. and White, J. M. in Proceedings of the XIX Solvay Conference, (Edited by F. W. deWette) Springer, New York, (1988), p. 343.
19. Liu, Z.-M., Akhter, S., Roop, B. and White, J. M. J. Am. Chem. Soc. **110**, 8708 (1988).
20. Germer, Th. A., Ho, W., J. Vac. Sci. Technol. **A7**, 1878 (1989).
21. Burgess, Jr. D., Mantell, D. A., Cavanagh, R. R. and King, D. S., J. Chem. Phys. **85**, 3123 (1986).
22. Burgess, Jr. D., Cavanagh, R. R. and King, D. S., J. Chem. Phys. **88**, 6556 (1988).
23. Buntin, S. A., Richter, L. J., Cavanagh, R. R. and King, D. S., Phys. Rev. Lett. **61**, 1321 (1988).
24. Hoheisel, W., Jungmann, K., Vollmer, M., Weidenauer, R. and Träger, F., Phys. Rev. Lett. **60**, 1649 (1988).
25. Natzle, W. C., Padowitz, D. and Sibener, S. J., J. Chem. Phys. **88**, 7975 (1988).
26. Weide, D., Andresen, P. and Freund, H.-J., Chem. Phys. Lett. **136**, 107 (1987).
27. Budde, F., Hamza, A. V., Ferm, P. M., Ertl, G., Weide, D., Andresen, P. and Freund, H.-J., Phys. Rev. Lett. **60**, 1518 (1988).
28. (a) Menzel, D. and Gomer, R., J. Chem. Phys. **41**, 3311 (1964); (b) Readhead, P. A., Can. J. Phys. **42**, 886 (1964).
29. Menzel, D., Nucl. Instr. Meth. **B13**, 507 (1986).
30. Menzel, D., in "Study of Surfaces and Interfaces by Electron Optical Techniques" (Edited by A. Howie and U. Valdre), Plenum Press, New York (1988).
31. Desorption Induced by Electronic Transitions, Diet III, Stulen, R. H., Knotek, M. L., (Eds.) in Springer Series in Surface Sciences **13**, Springer, New York, (1988).
32. Ferm, P. M., Budde, F., Hamza, A. V., Jakubith, S., Ertl, G., Weide, D., Andresen, P., Freund, H.-J., Surf. Sci., to be published.
33. Mull, Th. Dissertation, Bochum (in progress).
34. Koel, B. E., Peebles, D. E. and White, J. M., Surf. Sci. **125**, 709 (1983).
35. Dalmai-Imelik, G., Bertolini, J. C. and Rousseau, J., Surf. Sci. **63**, 67 (1977).

36. Cowin, J. P., Auerbach, D. J., Becker, C. and Wharton, L., Surf. Sci. **78** (1978) 545.
37. Cowin, J. P., Phys. Rev. Lett. **54**, 368 (1985).
38. Smedley, J., Corey, G. C. and Alexander, M. H., J. Chem. Phys. **87**, 3218 (1987).
39. Schönhammer, K. and Gunnarsson, O., Solid State Commun. **26**, 399 (1978).
40. Hermann, K., Bagus, P. S., Brundle, C. R. and Menzel, D., Phys. Rev. **B24**, 7025 (1981).
41. Freund, H.-J., and Plummer, E. W., Phys. Rev. **B23**, 4859 (1981).
42. Messmer, R. P., and Lamson, S. H., Chem. Phys. Lett. **65** 465 (1979).
43. Brundle, C. R. and Wandelt, K. Proc. 7th Int. Vac. Congr., Vienna, p. 1171 (1977).
44. Fuggle, J. C., Umbach, E., Menzel, D., Wandelt, F. and Brundle, C. R. Solid State Commun. **27**, 65 (1978).
45. Witzel, S. and Neumann, M., to be published; see also BESSY-Jahresbericht p. 197 (1988).
46. Odörfer, G., Kuhlenbeck, H. and Freund, H.-J., unpublished.
47. Stöhr, J. and Jaeger, R., Phys. Rev. **B26**, 4111 (1982).
48. Geisler, H., Diplomarbeit, Bochum (1989).